Chapter 4
Materials and Methods

Chapter 4

Materials and Methods

Based on the design dimensions of various components reported in Chapter 3, a prototype integrated drying system (IDS) was fabricated was fabricated at a cost of Rs.80,000/- and commissioned. Name of components fabricated and their specifications are listed in Table 4.1. Experiments were conducted to determine the optimum drying time, energy consumption, maximum temperature achieved, air flow rate, working of the control mechanisms, sequencing of trays and various quality attributes of the dried products. This chapter is presented under the following main headings:

I. Fabrication of various components of the IDS
II. Assembling of the IDS
III. Experimentation and observations
IV. Quality attributes
V. Statistical analysis
VI. Simulation and process optimization

Table 4.1 Specifications of different components of IDS

Sl. No.	Components	Specifications
1.	Solar collector	2220 mm x 1230 mm x 160 mm
2.	Collector absorber	1.5 mm thick black painted aluminum
3.	Collector insulation	5 mm Plywood board
4.	Collector surface	8 mm Pyrex glass
5.	Collector inclination	15^0
6.	Compound parabolic collector	6 nos: 1860 mm length ; spacing: 15 mm
7.	Combustion chamber	1620 mm (L) x 450 mm dia.
8.	Combustion chamber grate	1315 mm (L) x 305 mm (B)
9.	Flue gas chimney	3350 mm (H) x 200 mm dia.
10.	Husk feeding assembly	Grates:9 ; 25 mm (B)
11.	Husk feeding hopper	700 mm (W) x 220 mm (H)
12.	Grate inclination	$45^0 – 90^0$
13.	Drying chamber	1100 mm (H) x 1000 mm (W)
14.	No of trays (SS)	6 : 950 mm x 950 mm
15.	Freeboard	80 mm
16.	Wind turbine	230 mm collar dia.
17.	Hinged door	1100 mm (H) x 950 mm (W)
18.	Loading/unloading platform	1000 mm x 1000 mm at a height of 1150 mm

4.1 Fabrication of various components

Components of the IDS viz. solar collector; combustion chamber; hot air generation chamber; husk feeding assembly; chimney; drying chamber; drying trays; insulation work and loading-unloading facility were fabricated as per design.

4.1.1 Solar collector

The solar flat plate collector of dimension 2220 mm x 1230 mm x 160 mm was fabricated. The collector surface was fabricated of 1.5 mm thick black painted aluminum sheet with ply board insulation at the bottom. The 2 sides were fabricated from 18 gauge mild steel (MS) sheet with ply board insulation on the outer sides and painted black in the inner sides. The collector surface area was covered with 8 mm thick transparent glass Pyrex sheet of same dimension. The whole collector was mounted on 25 mm MS angle iron frame with four pairs of legs at an inclination of 15^0. The neck of collector was tapered to width 950 mm at the outlet. A flange of size 1030 mm x 240 mm was fabricated from 3 mm MS flat to eliminate hot air leakage by fitting properly with the inlet of the drying chamber. Heat resistant rubber gasket was cut into size and pasted on the face of the flange for better sealing. Temperature measuring ports were drilled near the outlet and inlet which were plugged with thermo cork plugs.

4.1.2 Compound parabolic collector

After initial rounds of experimentation, 6 numbers of compound parabolic concentrators were fabricated as per design of size 1860 mm in length and 1220 mm in breadth with 15 mm space between each. Interior surface of the parabolic reflector was made up of glazed aluminum sheet which reflected the solar rays on the face of a receiver placed at the focal position of the concentrator. Metallic tubes (6 numbers) of outer diameter 32 mm, thickness 15 mm and length of 1860 mm were painted black and placed as receivers along the focus and fitted inside the glass cover (Fig. 4.1).

4.1.3 Sun tracking facility

As the sun moves away from the vertical and the solar azimuth increases, the intensity of receiving energy also gets reduced. A manual sun tracking flexibility was incorporated. A chute made up of water proof canvas of size equal to the flange was

stitched and fitted between the dryer chamber and collector to enable horizontal and vertical directional change of the receiver by 11.54^0 and 4.68^0 , respectively.

4.1.4 Combustion chamber

The combustion chamber of dimension 1620 mm in length and 450 mm in diameter was fabricated from 16 gauge thick MS sheet. The cylinder was made to rest on 3 pairs of legs made from 50.8 mm angle iron so as to give elevation of 780 mm from the bottom (Fig.4.2). The exhaust end of the combustion chamber was connected to a chimney for necessary draft creation and exit of flue gas. As shown in the figure, the combustion chamber was placed inside a chamber fabricated from MS sheet with two air inlets at the bottom and an outlet port on opposite of inlet side. A baffle plate was fixed in the out let for air flow control. A layer of rock was placed at the bottom for better heat retention. Over the cylinder, iron scraps were laid to increase heat transfer area and air residence time. Sliding type closing and opening plate was provided in the ambient air ports for inlet air flow control. The ambient air entering into the chamber gets heated while in contact with the hot combustion chamber surface and gets sucked into the bottom of the drying chamber due to natural convection and draft created by the wind turbine fitted on top of the drying chamber.

A horizontal grate of size 305 mm in width and 1315 mm in length with openings of size 50 mm x 50 mm was made and placed inside along the length of the combustion chamber for proper burning while using woody biomass as fuel. The chimney end of the chamber was made detachable for inspection and ease of maintenance in due course of time. As per design calculations a chimney of 3350 mm height and 200 mm diameter was made from mild steel sheet and fitted to the combustion chamber. A conventional rain guard was fitted over the chimney.

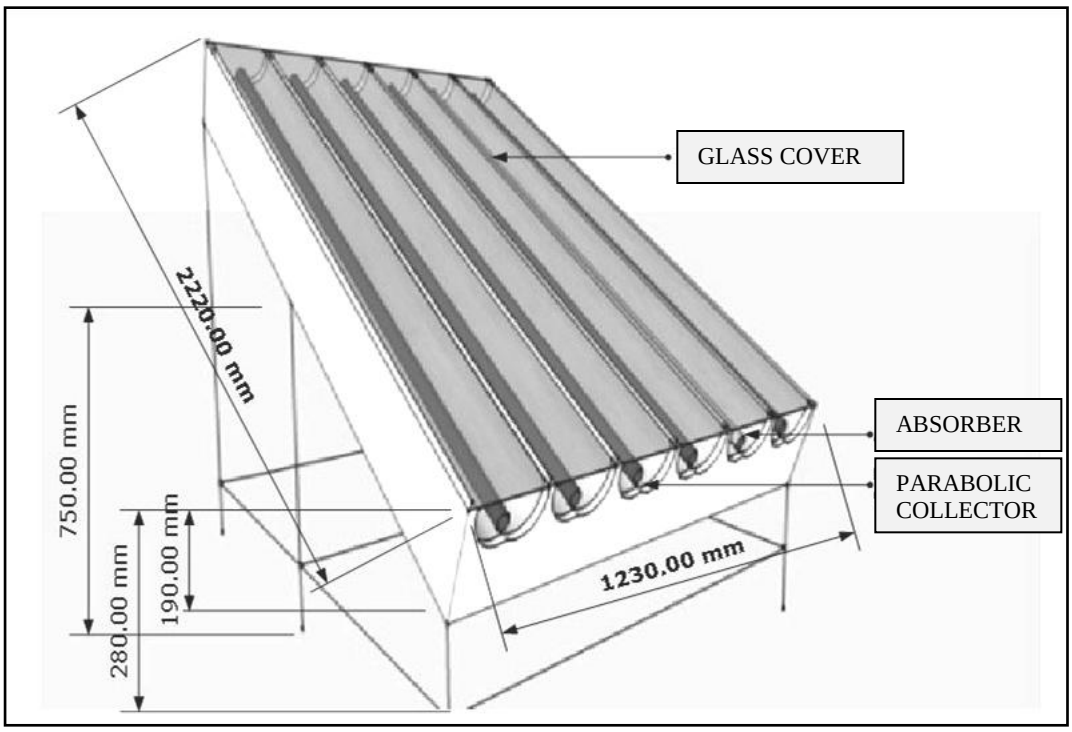

Fig. 4.1 Schematic of CPC

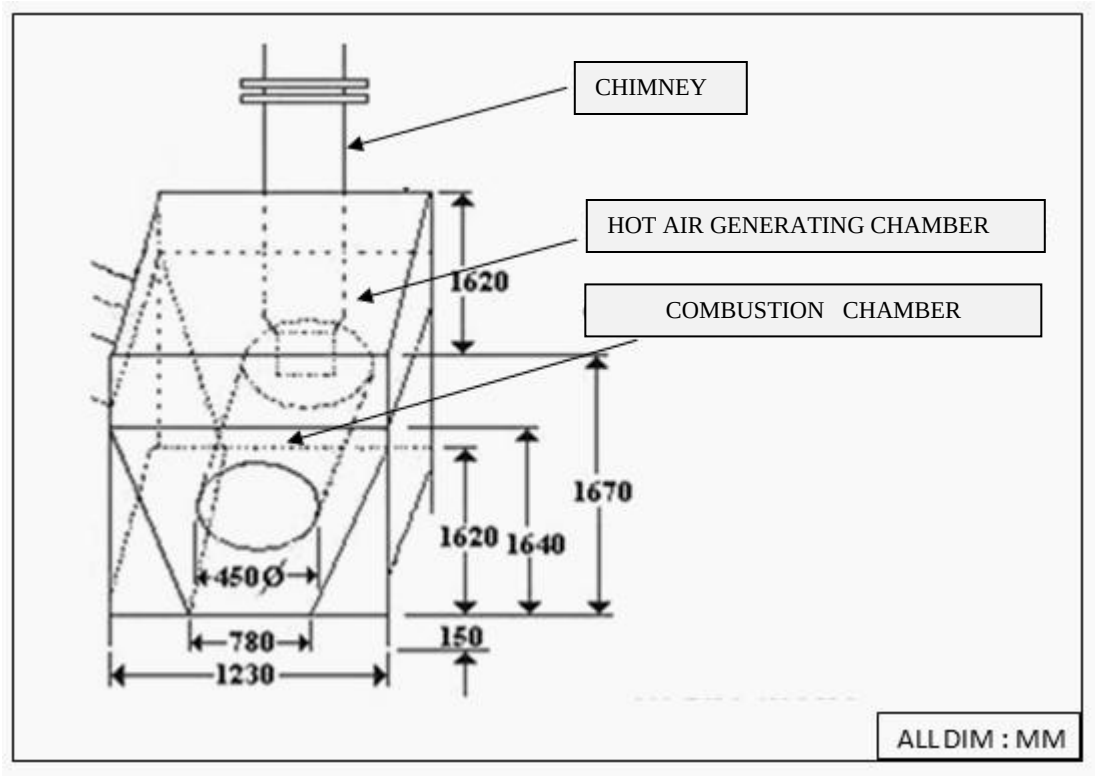

Fig. 4.2 Schematic of combustion chamber

4.1.5 Feeding device

For feeding of paddy husk into the combustion chamber, an inclined grate type feeding mechanism with hopper was fabricated. A total of 9 grates of 25 mm width welded to 10 mm rods were fixed to flat iron strips on both sides (Fig.4.3 and Fig.4.4). The arrangement was made in such a way so that by stroking the flat iron through the liver provided, the inclination of the grates altogether could be increased or decreased between $45^0 – 90^0$. This was done to ensure sufficient inflow of air for proper burning and smooth flow of husk from the hopper to the combustion chamber. A fluted type feeding system was fabricated and used in the hopper for controlled flow of husk to ensure continuous combustion. The whole husk feeding system was mounted on a separate angle iron frame for easy detachment from the main chamber. Thus, the unit became versatile for use of solid bio-waste or paddy husk as the case may be. A semicircular MS sheet of diameter same as the combustion chamber was made available to reduce the opening of the air inlet below the bottom most grate to ensure proper air flow only through the grates and not through any other ways, while paddy husk was used as fuel. A half-moon shaped scooper was fabricated of MS material to scoop out burnt ashes falling to the bottom of the combustion chamber through the grate openings.

4.1.6 Drying chamber

The drying chamber consisted of plenum chamber, drying chamber, free board and exhaust. This part was fabricated from 1.29 mm MS sheet welded to the main frame (Fig.4.5) fabricated from 25 mm x 38 mm tubular pipes. A total of 6 trays were fabricated using SS sieves and GI side bunds as per design specifications. From the top most trays, a free board of 80 mm depth was provided beyond which the chamber was made tapered upwards to fit into a round collar of diameter 375 mm. A wind turbine having collar diameter 380 mm was procured readymade and fitted over the chamber by tightening 3 screw bolts.

A hinged door of size 950 mm x 1100 mm was fabricated and fitted to front side of the drying chamber. The trays were made to slide in the tubular pipes and closed shut by the door. Thermal gasket was cut to size and pasted inside the door periphery to prevent air leakage.

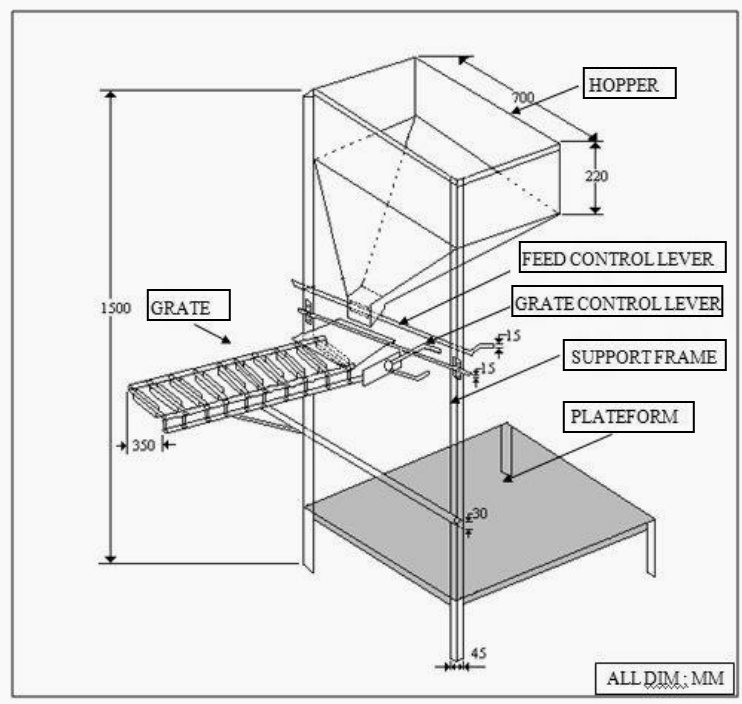

Fig. 4.3 Husk feeding arrangement

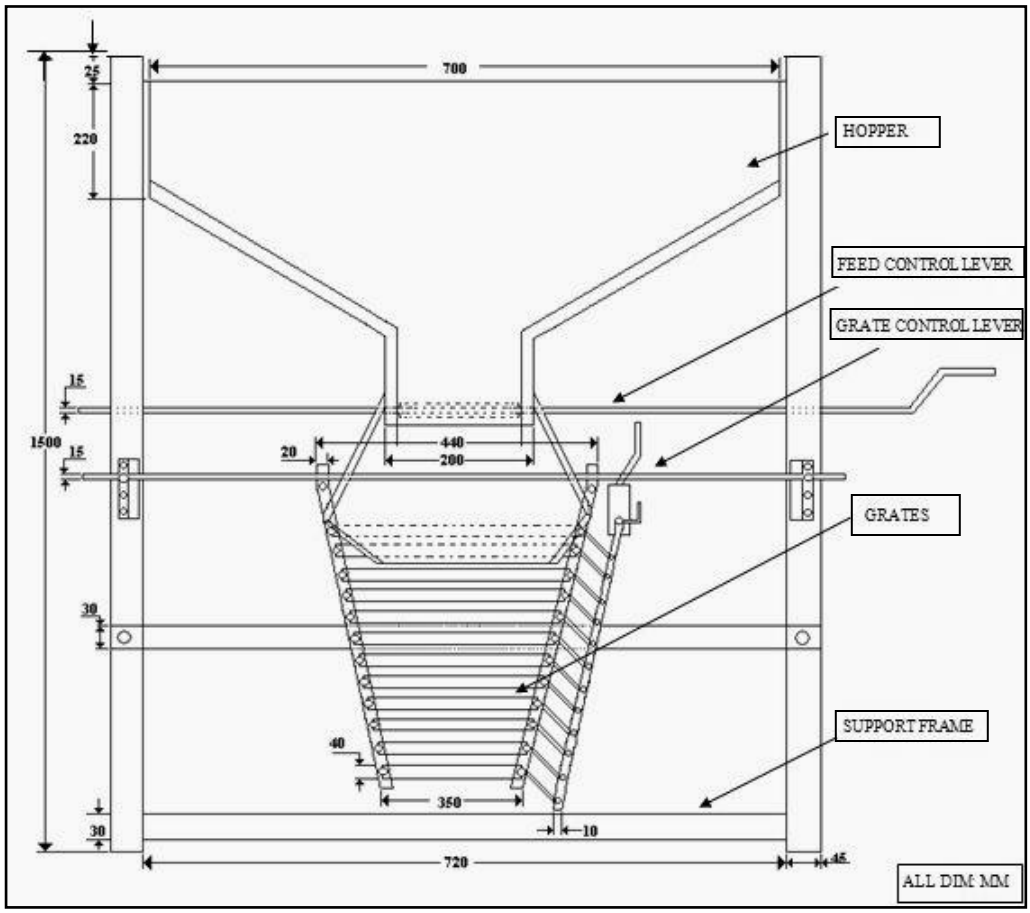

Fig. 4.4 Husk feeding arrangement side view

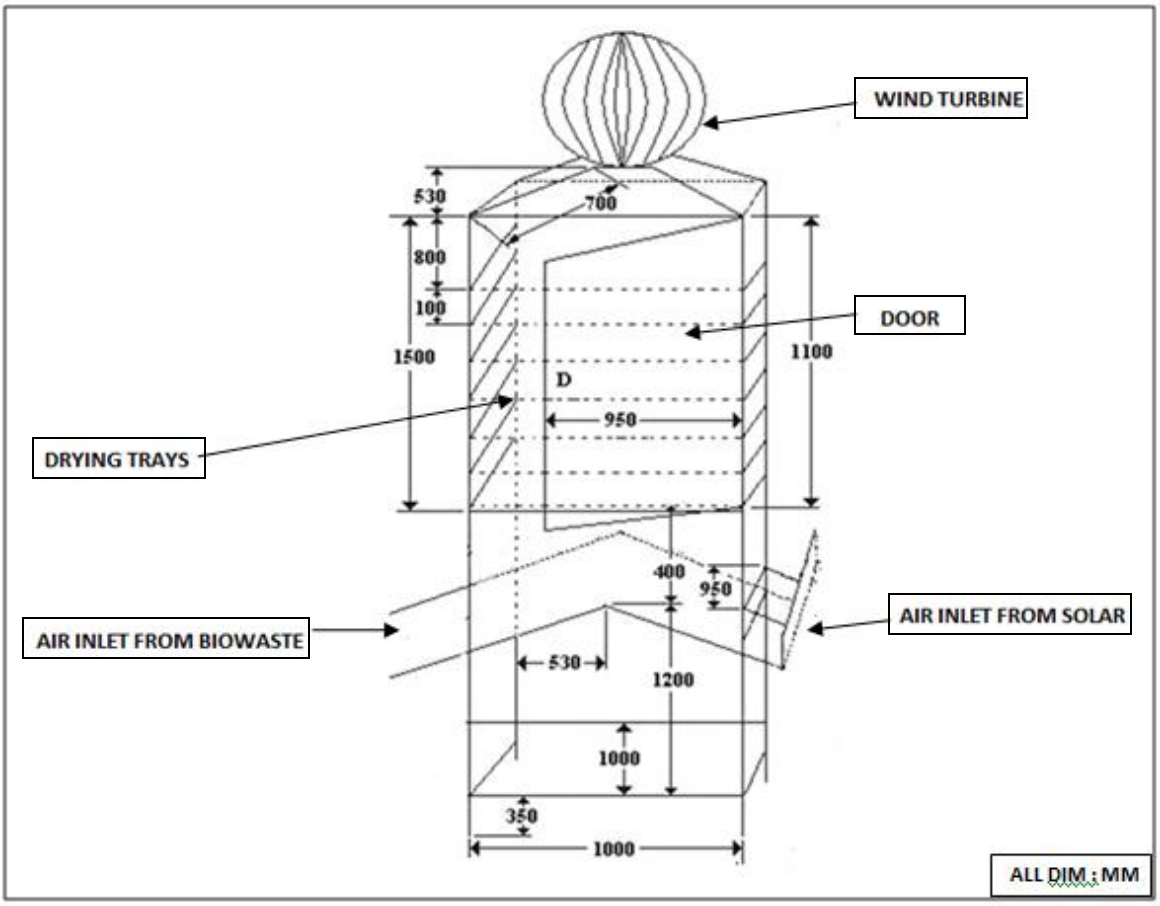

Fig. 4.5 Drying chamber

4.1.7 Control mechanisms and measuring ports

Two MS sheets of size 945 mm x 185 mm were cut. MS rod of 5 mm diameter and of 1100 mm length was welded on each sheet along the length. One end of the rod was bent into L-shape to form a handle. The whole arrangement was finally made into half turn butterfly dampers for air flow regulation and was fixed on the necks of hot air inlets.

To control flow of flue gas through chimney, a circular butterfly valve was made and fitted inside the chimney with a control lever to provide movement. The butterfly valve could be operated to position itself between full to minimum opening for draught control in the chimney.

To increase or decrease the residential time of ambient air entering the hot air generating chamber two sliding gates were provided to one side of the chamber near to the

bottom. Temperature measuring ports were provided at the dryer inlet and exit. Near to the top of the dryer and hot air inlet, measuring slots were provided to measure air velocity using anemometer.

4.1.8 Loading and unloading

Provision for loading and unloading for raw materials was facilitated from the front. A single pan door made of MS sheet, double layered was made. Three door hinges were provided with two latch lock on the opposite side for firm closing of the door. After opening the door to 90^0 or more the trays could be slide out. A support of size same as width of the tray shaped as a 'T' made from MS pipes with adjustable height was provided to give support to the pulled out trays while loading and unloading. A platform of size 1000 mm x 1000 mm at a height of 1150 mm from ground level with an iron ladder was fabricated from MS sheet, angle iron and MS pipes.

4.1.9 Insulation work

The hot air generating chamber of the bio-waste fired unit excluding the fuel feeding side, all faces of the drying chamber and sides were first covered with 5 mm thick particle boards. The surfaces were then laminated with commercial grade black polythene sheets to protect from rain water. Insulation to the solar collector bottom was done by covering with ply board and oil painted for durability.

4.2 Assembling of the IDS

The hot air generating parts were attached to the drying chamber from two sides fixed through flanges. Temperature resistant gaskets were pasted between the flanges to make the joining air tight. The fuel feeding side of the bio-waste fired unit and loading-unloading side of the drying unit were placed as front of the drying system. To the right of the dryer the solar part was attached through a flexible neck made up of water resistant canvas cloth. This was done to enable tracking of the sun during second half of the day. The final design drawing of the IDS is given in Fig.4.6.

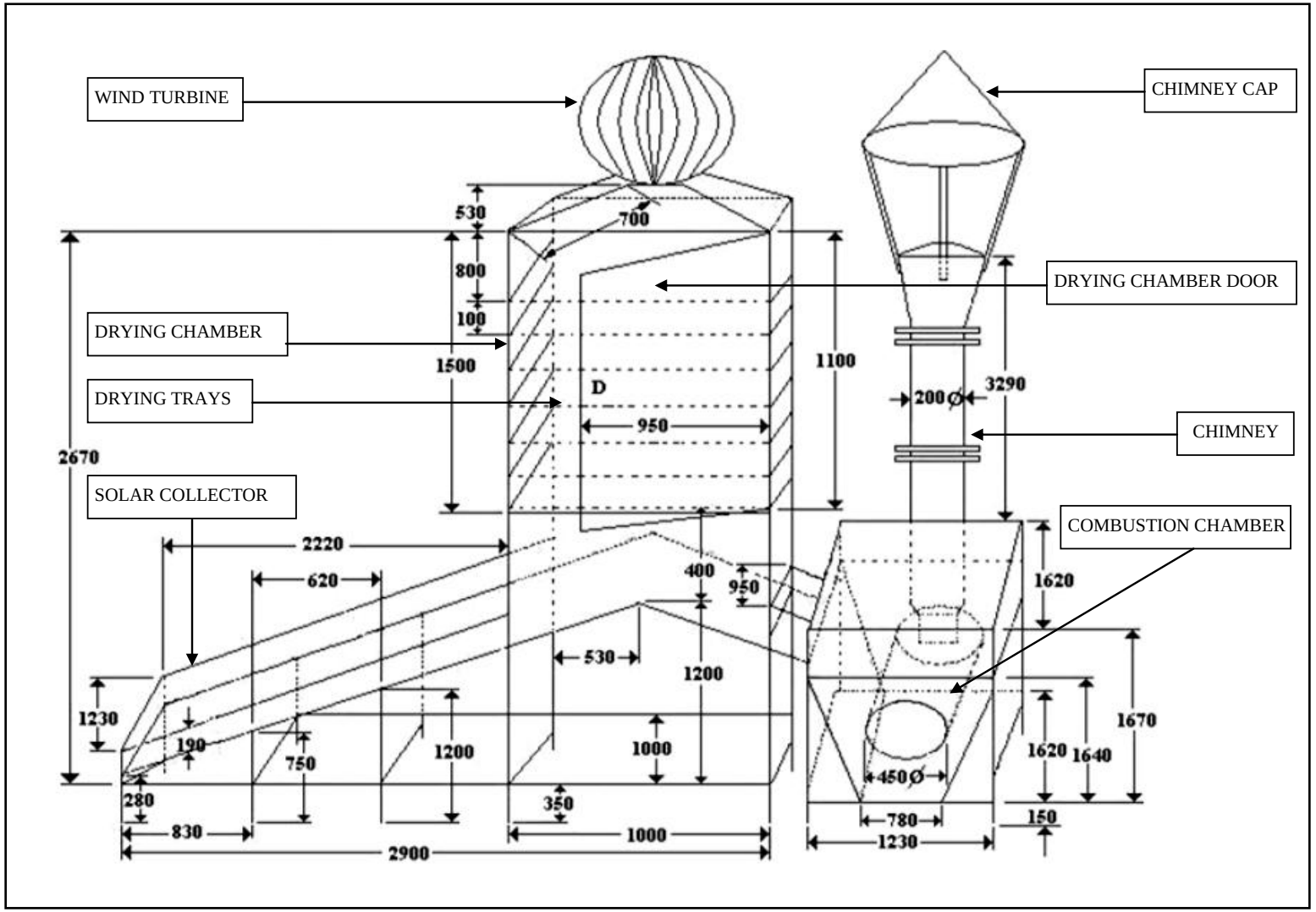

Fig. 4.6 Schematic of the Integrated Drying System (all dimensions are in mm)

4.3 Experimentation and observations

The developed integrated drying system after completion of fabrication commissioned for experimentation (Fig. 4.7; Fig. 4.8 and Fig. 4.9). Raw ginger and turmeric rhizomes were procured and washed with tap water to remove dirt. Surface water was removed by centrifuging in a basket centrifuge (Fig.4.10). Ginger rhizomes were sliced into 3 - 4 mm thickness and 50-70 mm in length manually and spread on the trays in thin layers. For turmeric, rhizomes were cut into same sizes as for ginger but pretreated with boiling water for 2 minutes before slicing (Prasad *et al.*, 2006). The drying was carried out initially with solar drying alone to remove the initial moisture followed by drying with bio-waste fired dryer up to the end of drying. Initial weight of samples and moisture content was measured and recorded using digital moisture balance (Fig.4.11) CB-50 (Contech Instrument Limited).

Temperature of drying air was measured near the air inlet of the drying chamber in the respective sides of solar and bio-waste fired sources by J-type thermocouples. Temperature of exhaust air was measured immediately below the wind turbine at the top. The air velocity was measured with a velocity transmitter (Fig.4.12) of Make-Kimo Instrument, France. All the measuring instruments were logged into a 16-channnel data logger (Make-R.S. Process System Pvt. Ltd., India) (Fig.4.13). Weight of fuel burnt during drying was recorded. Initial time was recorded after attaining a steady temperature by the hot air. Trays were rotated as per predetermined sequence to achieve uniform drying.

Temperature, moisture content of the samples and weight loss was monitored regularly using temperature probes (Fig.4.14), to know the end of drying keeping track tray wise. The trays were interchanged in a clockwise sequence and the materials were stirred at 1-h interval (Chua and Chou, 2003). Simultaneous open sun drying of samples was carried out from the same lot of raw material, as control. Intensity of solar radiation data were collected from Meteorology Dept. of Assam Agricultural University, Jorhat. Along with the developed dryer, drying were also carried out simultaneously in a fluidized bed dryer (FBD), electrical oven and open sun drying for comparison. Open sun drying which is the common practice was taken as control.

Fig. 4.7 Side view of the drying system

Fig. 4.8 Combustion Chamber

Fig. 4.9 Front view of the drying system

Fig. 4.10 Basket centrifuge

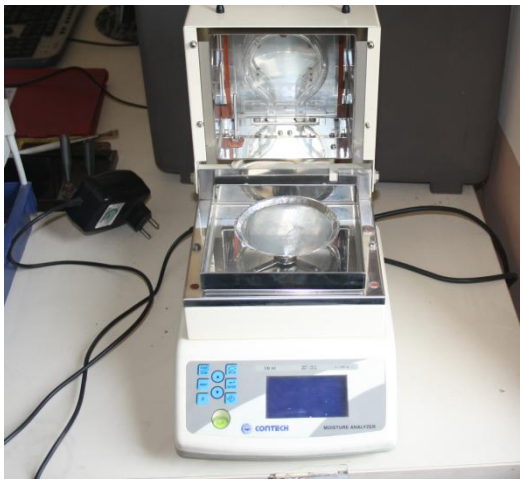

Fig. 4.11 Moisture balance

Fig. 4.12 Air velocity transmitter

Fig. 4.13 Data logger

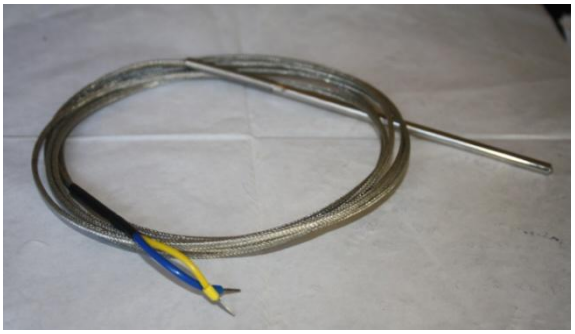

Fig. 4.14 J-type thermocouple

4.4 Quality attributes

To understand the effect of selected drying methods on the quality aspects of dried spices, analysis were done for different parameters viz. rehydration ratio, oleoresin level, volatile oil content, texture, colour for ginger samples and curcumin content, texture, colour for turmeric samples. All data were recorded in five replications before taking average values.

4.4.1 Texture analysis

Texture or firmness of the dried samples was measured using a texture analyzer (SMS-TA-XT2, Stable Microsystems Ltd., Godalming, Surrey, United Kingdom) with a 100 kg load cell which was equipped with a 3 mm diameter cylindrical stainless steel probe. Texture was calculated as peak force (g) measuring resistance to the compression imposed by the sample to the metal probe (Mishra *et al.*, 2004). Maximum stress or hardness was defined as the maximum peak force (Moreira *et al.*, 2008) and reported the average of three trials. The toughness is often taken as the total positive area under the curve. This measurement effectively records the total 'work' involved in performing the test. It therefore follows that a higher area value indicates a higher amount of energy involved in performing the test and subsequently is translated as a tougher sample to test. Thus, average of positive area under curves during each measurement was recorded to understand toughness. The cross head speed was fixed at 10 mm/s. The instrument shown in (Fig.4.15) was calibrated before the test. The texture of dried products (approximate 5-g piece) was determined in 5 replicates for each samples from sun dried, fluidized bed dryer, electrical oven and tray wise for integrated dryer.

4.4.2 Rehydration characteristics

Rehydration studies were carried out for ginger as, while used for culinary purposes it is expected to be soft. The dried samples (15 g each) were soaked in distilled water (300 ml) at room temperature. Data were recorded every 30 minutes interval up to 150 minutes of soaking. Care was taken to blot the superficial water every time before data was recorded. The rehydration characteristics were studied in terms of:

a. Rehydration ratio (RR)—Ratio of weight of rehydrated sample to that of dehydrated sample.

$$RR=\frac{W_2}{W_1} \quad \text{---------- (4.1)}$$

b. Coefficient of rehydration (COR) (Ranganna, 1991)

$$COR = \frac{W_2 \times (100 - M_I)}{(W_1 - M_F) \times 100} \quad \text{----------(4.2)}$$

where, W_2 is the drained weight of dehydrated sample; W_1 the weight of dried sample taken for rehydration; M_1 the moisture content of sample before drying; M_F the amount of moisture present in dried sample taken for rehydration.

4.4.3 Colour evaluation

Colour of fresh, dried and rehydrated ginger was observed from all the drying methods using the MiniScan XE Plus model colorimeter (Hunter Lab) manufactured by Hunter Associate Laboratories Inc., Virginia, USA. Out of five available colour systems, the L*a*b* (Maskan, 2001b; Krokida *et al.*, 1998; Lozano and Ibarz, 1997) system was selected as it is the most widely used system for colour evaluation of dried food materials (Fig. 4.16). Before taking actual reading of the sample, the colorimeter was calibrated with a standard white tile (L^*= 93.96, a^*=−1.08,b^* =0.40) supplied with the instrument. The sample pieces were covered with thin transparent polyethylene sheets to prevent fogging of the lenses from the moisture present in the samples. The samples were placed in the colourimeter in such a way that all the light falls on and is reflected back from the sample only. The colour values were represented on the CIE (Commission Internationale de l'Eclairage) colour scales as L^* (lightness / darkness), a^* (redness / greenness) and b^* (yellowness / blueness) and standard illuminant D_{65} and observer 2^o. The CIE system characterizes colours by a luminance parameter Y and two colour coordinates ‘x’ and ‘y’, which specify the point on the chromaticity diagram.

Total colour change, DE*, was then calculated by using following equation (Gowen *et al.*, 2008):

$$DE^*=\sqrt{(L^* - L_0^*)^2+(a^* - a_0^*)^2 + (b^* - b_0^*)^2} \quad \text{----------(4.3)}$$

Where L_0^*, $a_0^*$and b_0^* refer to the CIE colour values for fresh as well as treated samples from each drying methods.

The overall change in colour (DE*), relative changes in Hue and Chroma of different samples with respect to that of fresh were calculated to estimate variation in sample colour (Sigge *et al.*, 2001).

$$\text{Hue} = \tan^{-1}\left(\frac{b_0^*}{a_0^*}\right) \quad \text{----------(4.4)}$$

$$\text{Chroma} = \sqrt{(a_0^{*2} + b_0^{*2})} \quad \text{----------(4.5)}$$

4.4.4 Oleoresin content

Oleoresin content of dried ginger was determined as per the method of oil extraction using a Soxhlet extraction apparatus (AOAC'1970). An accurately weighed (5gm) sample was taken in cellulose thimble and the mouth plugged with cotton. Extraction was done with petroleum ether (boiling point 40-60 ^{0}C) for 8-16 h in a Soxhlet apparatus (Fig.4.17). After removal of ether by evaporation, the residue was dried in an oven at 80^0 C, cooled in desiccators and weighed. The average value of five samples was taken for calculation of oleoresin percent on moisture free basis using the following standard expression.

$$\text{Oil and fat \%} = \frac{\text{Wt. of the ether extract} \times 100}{\text{WeightofSample}} \text{----------(4.6)}$$

4.4.5 Volatile oil content

Hydro-distillation method was adopted. Ginger oil or volatile oil was extracted from dried ginger powder using Clevenger Steam distillation apparatus (Fig. 4.18). Ground sample of 50g was accurately weighed and taken in a round bottom flask and distilled water (500 ml) added and heated to boiling (80-90^0 C). The volatile oil got collected above condensed vapor within 1-2 h and was withdrawn from the graduated burette (Purseglove *et al.*, 1981).

4.4.6 Curcumin evaluation

Curcumin the principle curcuminoid of turmeric is responsible for its yellow colour and serves as measure of turmeric quality. The value of a particular turmeric cultivar is determined on the basis of its curcumin content.

The extraction and estimation of curcumin was carried out by adopting method given by Shadasivam and Manikam (2008). Curcumin was quantitatively extracted by refluxing a measured quantity of dried sample powder with alcohol and was estimated by Spectrophotometric method at 425 nm wavelength using double beam Spectroscan UV-2700 (Chemito make) spectrophotometer (Fig.4.19).

For this purpose, (0.2 - 0.5gm) 0.4gm moisture free dried sample was dissolved in 250 ml of 95% (absolute) alcohol. Refluxed the content in the flask fitted with an air condenser over a heating mantle for 3-5 hrs, compensated alcohol in to the flask, subsequently cooled the extract and decanted to a 250 ml volumetric flux and made up the volume. Finally diluted the (1-2 ml) supernatant aliquot with 9 ml alcohol and measured the curcurmin at 425nm wavelength in spectrophotometer. Following formula was used to estimate curcumin content:

$$\text{Content } \% = \frac{0.0025 \times A_{425} \times \text{Volume made up} \times \text{dilution factor} \times 100}{0.42 \times \text{weight of the sample (g)} \times 1000} \quad \text{---------(4.7)}$$

(0.42 absorbance at 425 nm = 0.0025 g curcumin)

Curcumin of each sample was also estimated by using standard curcumin. Pure curcumin was acquired from E-Merck. For standard graph, 5 mg of standard curcumin was diluted in 50 ml of 95% alcohol and from that 50 µl, 100 µl, 200 µl, 400 µl, 600 µl, 800 µl, 1 ml, 2 ml, 5 ml, 6 ml, respectively in each test tube and readings were taken at 425 nm by spectrophotometer.

Fig. 4.15 Texture analyzer

Fig. 4.16 Colorimeter

Fig. 4.17 Soxhlet apparatus

Fig. 4.18 Clevenger apparatus

Fig. 4.19 Spectrophotometer

4.4.7 Statistical analysis

Results obtained of ginger and turmeric samples dried in the selected methods were statistically analyzed using 1-way analysis of variance (ANOVA) test to estimate the significant difference between different drying methods. The parameters considered for the analysis were overall change in colour (ΔE-value), rehydration characteristics (RR), texture, oleoresin and volatile oil of ginger, curcumin content of turmeric.

4.5 Simulation and process optimization

As per Spices Board of India report (Anonymous, 2006) production of ginger (138370 M.T) and turmeric (20360 M.T) is quite significant in the North East region of India and have high intrinsic values. Optimization of drying process for the dryer was thus carried out considering these spices.

4.5.1 Simulation of drying process

Simulation of the drying method was done by using different thin layer drying models that are based on the moisture ratio of samples. Tray wise moisture content data were converted into the moisture ratio (MR) expressions and curve fitting with drying time for the selected drying models were analyzed. The different thin layer drying models considered are given in Table 4.2.

Table 4.2 Different drying models

Sl.No.	Name of Model	Model Expression	Reference
1	Lewis	$MR = \exp(-kt)$	(Lewis, 1921)
2	Page	$MR = \exp(-kt^n)$	(Loha *et al.*, 2012)
3	Modified Page	$MR = \exp[-(kt)^n]$	(Overhults *et al.*, 1973)
4	Henderson and Pabis	$MR = a \exp(-kt)$	(Henderson and Pabis, 1961)
5	Logarithmic	$MR = a \exp(-kt) + b$	(Yaldiz and Ertekin, 2001)
6	Wang & Singh	$MR = a + bt + ct^2$	(Wang and Singh, 1978)

Representation of different symbols:

MR - moisture ratio;
a, b, c, n - constants;
k - drying rate constant
t - drying time in hour.

MR was obtained using the following expression:

$$MR = \frac{M - M_e}{M_0 - M_e} \quad \text{---------- (4.8)}$$

Where, M is the material moisture content at time t in % (wb); M_e is the material moisture content in equilibrium with drying air temperature in % (wb) and M_0 is the initial moisture content % (wb) of the material.

Experimentally obtained drying curves for six different trays were fitted with the six different MR models. Sigma Plot (Version 11.00) statistical software was used to analyze the data obtained during drying and for mathematical modeling of drying curves (Jayashree and Visvanathan, 2013). The coefficient of determination (R^2) was selected as one of the primary criteria to select the best equation to account for variation in the drying curves of dried samples (Diamante *et al.*, 2010). In addition to this, suitability of these equations was evaluated in terms of statistical parameters such as mean percentage error (P) and standard error estimate (SEE). Higher values of R^2, lower values of P and SEE were chosen as the criteria for goodness of fit of the curve to the equations (Basunia and Abe, 1999). These parameters could be found as:

$$R^2 = \frac{\sum_{i=1}^{N}(MR_{exp,i} - MR_{exp\ mean,i})^2 - (MR_{pre,i} - MR_{exp,i})^2}{\sum_{i=1}^{N}(MR_{exp,i} - MR_{exp\ mean,i})^2} \quad \text{----------(4.9)}$$

Where, $MR_{exp,I}$ stands for the experimental moisture ratio found in any measurement, $MR_{pre,i}$ is the predicted moisture ratio for this measurement and N is the total number of observations.

Standard error of estimate (*SEE*) provides information on the long term performance of the correlations by allowing a comparison of the actual deviation between predicted and measured values, term by term. The ideal value of *SEE* is "zero".

$$SEE = \sqrt{\frac{\sum_{i=1}^{N}(MR_{exp,i} - MR_{pre,i})^2}{N - n_i}} \quad \text{---------- (4.10)}$$

Where, n_i is the number of constants.

Mean, percentage error,

$$P = \frac{100}{N}\sum_{i=1}^{N}\frac{(MR_{exp,i} - MR_{pre,i})^2}{MR_{exp,i}} \quad \text{----------(4.11)}$$

4.5.2 Effective moisture diffusivity:

Following Fick's second law, the moisture diffusion during drying of ginger spread in the form of thin slabs as follows (Crank, 1975):

$$MR = \frac{8}{\pi^2}\left[\sum_{n=1}^{n=\alpha}\frac{1}{(2n+1)^2}exp\left(\frac{-(2n+1)^2\pi^2 D_{eff}\, t}{4h^2}\right)\right] \text{---------- (4.12)}$$

For long drying hours, by taking n = 0 (Geankoplis, 2003) it could be reduced to:

$$MR = \frac{M - M_e}{M_0 - M_e} = \frac{8}{\pi^2}\exp\left(\frac{-\pi^2 D_{eff}\, t}{4h^2}\right) \quad \text{---------- (4.13)}$$

Where, D_{eff} is the effective moisture diffusivity, m^2h^{-1}, 't' is the drying time in hours and 'h' is the thickness in 'm' of infinite slab dried from top and bottom parallel surfaces.

The equation (4.13) could be rewritten as,

$$MR = Ae^{-kt} \quad \text{---------- (4.14)}$$

Where, the constants are, $A = \frac{8}{\pi^2}$, and $k = \frac{\pi^2 D_{eff}}{4h^2}$

Simplifying it to in linear form,

$$\ln(MR) = \ln\left(\frac{M - M_e}{M_0 - M_e}\right) = lnA - kt \quad \text{---------- (4.15)}$$

A plot of ln(MR) versus drying time gives a straight line with a slope (S). Assuming that drying occurs from top and bottom parallel faces, thickness of the slab to be dried from one face was assumed to be half of the total thickness 'h' in meter. The effective moisture diffusivity of ginger was calculated using the slope as,

$$k = \frac{\pi^2 D_{eff}}{4h^2} \quad \text{---------- (4.16)}$$

4.5.3 Optimization of drying process

The drying process was optimized based on texture, oil and oleoresin content, colour parameter, rehydration ratio of the dried ginger as well as energy consumption and drying time required in the above drying processes. In case of turmeric, curcumin level was additionally considered and no rehydration studies done as turmeric is eventually used in powdered form.

A nine point scale (on par with a nine point hedonic scale) was given to drying time, texture, oil content, colour parameter, rehydration and energy consumption in drying processes (Kaleemullah and Kailappan, 2005). Rehydration ration (RR) and COR values were considered for ginger experiments only as turmeric does not demand rehydration and only dried for grinding. The nine point scale was fixed based on the above drying experimental maximum and minimum values of the drying time, oil content, colour value, energy consumption and rehydration. Required drying hour was recorded for each drying process and maximum score was given to minimum drying time taken by the process to get a constant value of moisture content.

The colour of fresh and dried rhizome samples which were measured by Hunter Lab colorimeter, relative changes in Hue and Chroma of different samples with respect to that of fresh were calculated to estimate variation in sample colour. Minimum value thus obtained was given highest score while optimization.

The optimization among the dried herbs from the individual drying processes was carried out by analyzing the peak force required to penetrate the samples while using the texture analyzer instrument (Lasekan *et al.*, 2012). Harder texture of the dried product is a negative attribute. Hence, maximum force required for penetration was given minimum score.

From the energy consumption point of view, the processes were studied on specific energy requirement basis. The score was given to all the drying processes based on energy requirement for removal of unit weight of moisture.

Finally the one that scored the highest total from all the scales was considered as the optimal one.